FABRICATION OF LEAD SULFIDE (PbS) NANOSTRUCTURES FOR SOLAR CELL APPLICATIONS

By

AHMED SALMAN OBAID AL-QAYSSIE

Thesis submitted in fulfillment of the requirements for the degree of

Doctor of Philosophy

November 2013

DEDICATION

I dedicate this thesis to our first teacher, Prophet Muhammad bin Abdullah (Peace be upon him) who is the envoy of mercy to the worlds, and who has lead mankind out of darkness of disbelief and polytheism into light of belief in the oneness of Allah Almighty. I also dedicate this thesis to the souls of my father and mother. May Allah make this work in the balance of their good deeds.

With respect

ACKNOWLEDGEMENT

"All praises and thanks to ALLAH"

In the name of Allah, Most Gracious, Most Merciful, First and foremost, I thank the Almighty Allah for giving me inspiration, patience and health to complete this doctoral study.

I am deeply indebted to Professor Dr. Zainuriah Hassan, my supervisor who guided me and motivated me throughout the stages of doing this study. She has been instrumental in turning my dream into reality through her valuable guidance and constructive comments. I would like to extend my gratitude to Universiti Sains Malaysia for providing me with the financial support for carrying out this research. Also, I would like to express my gratitude to the School of Physics, Universiti Sains Malaysia. My appreciation also goes to the staff in the Nano Optoelectronics Research and Technology Laboratory for their co-operation, technical assistance and valuable contribution to my work. In addition, I would like to thank Dr. M. Bououdina from Nanotechnology Centre Manager, University of Bahrain for his help and good discussion. Special thanks are due to all my colleagues for their feedback and encouragement. I am what I am, because of my family: my brother Mohammed, Ammar, Thair, Ali , and my sisters. Last, and most important, I extend special thanks to my wife and my children (Ezzulddin and Mohammedulameen) who accompany me during this important time in our lives. Without their endless love, patience and support, I could not have a chance to complete this study.

Ahmed Salman Obaid Alqayssei.

Penang, Malaysia. May 2013

TABLE OF CONTENTS **Page**

LIST OF FIGURES

LIST OF TABLES

LIST OF SYMBOLS

A	Lattice constant
A	Absorbance
D	Interplanar spacing of the crystal planes
C_s	Average crystal size
E	Charge of electron
E_C	Conduction band
E_F	Fermi level of semiconductor
E_g	Semiconductor band gap
E_v	Valence band edge
(hkil)	Miller indices
I	Current
I_o	Saturation current
I_{sc}	Short-circuit current
J_{sc}	Current density
K	Boltzmann constant
m_o	Electron mass
m^*	Effective mass
m_e	Electron effective mass
m_p	Hole effective mass
N_c	Effective density of states
p	Free hole concentration
q	Electron charge
R	Reflectance
R_H	Hall coefficient

R_s	Series resistance
R_{sh}	Shunt resistance
T	Transmittance
t	Time
t	Thickness
T	Absolute temperature
V	Voltage
V_{oc}	Open-circuit voltage
V_m	Maximum voltage
V_H	Hall voltage
ν	Frequency
θ	Incident / Diffraction angle
χ	Semiconductor electron affinity
$\emptyset_B$	Schottky barrier height
ϕ_M	Metal work function
ϕ_S	Semiconductor work function
μ_n	Electron mobility
μ_p	Hole mobility
ρ	Resistivity
λ	Wavelength
FF	Fill factor
η	Solar cell efficiency

LIST OF MAJOR ABBREVIATIONS

a.u.	Arbitrary unit
AFM	Atomic force microscopy
CB	Conduction band
CBD	Chemical bath deposition
ECD	Electrochemical deposition
EDX	Energy dispersive X-ray
eV	Electron volt
FWHM	Full width at half maximum
I-V	Current-voltage
M	Metal
MACBD	Microwave assisted chemical bath deposition
MBE	Molecular beam epitaxy
MESFET	Metal-Semiconductor FET
MOCVD	Metalorganic chemical vapor deposition
Rms	Root mean square
SBH	Schottky barrier height
SC	Semiconductor
Sccm	Standard cubic centimeters per minute
SEM	Scanning electron microscope
TE	Thermal evaporation
UV	Ultraviolet
VB	Valence band
XRD	X-ray diffraction

FABRIKASI STRUKTUR NANO PLUMBUM SULFIDA (PbS) BAGI APLIKASI SEL SOLAR

ABSTRAK

Tujuan utama kerja-kerja penyelidikan yang dibentangkan dalam tesis ini adalah untuk mensintesiskan lapisan penyerap PbS berstruktur nano untuk peranti sel solar menggunakan kaedah yang mudah dan ekonomi: pemendapan rendaman kimia (CBD), pemendapan rendaman kimia berbantukan gelombang mikro (MACBD) dan penyejatan terma (TE). Sintesis lapisan PbS berstruktur nano menggunakan CBD telah dijalankan dengan menukar sumber ion Pb^{2+}, masa pemendapan, dan kepekatan molar. Hasil kajian menunjukkan bahawa ciri-ciri morfologi dan skala saiz PbS berstruktur nano sangat bergantung pada setiap parameter. Analisis pembelauan sinar (XRD) mendedahkan bahawa filem nipis PbS berstruktur nano mempamerkan struktur jenis garam batu kubus (NaCl). Keadaan optimum untuk sintesis PbS berstruktur nano menggunakan CBD adalah plumbum nitrat sebagai sumber ion Pb^{2+} dengan kepekatan molar 0.1 M. Sampel PbS dengan keadaan optimum telah dipilih untuk digunakan sebagai lapisan penyerap pada peranti sel solar PbS/CdS/ITO.

Selepas itu, PbS berstruktur nano dimendapkan menggunakan MACBD di bawah keadaan yang berbeza: mengubah sumber ion Pb^{2+}, mengubahkan masa pemendapan dalam lingkungan 30 hingga 90 minit, dan kepekatan molar. Analisis mikroskopi imbasan elektron (SEM) menunjukkan bahawa setiap parameter mempunyai kesan ke atas perubahan morfologi. Analisis struktur hablur oleh XRD mengesahkan pembentukan fasa tunggal kubik dengan jenis garam batu (NaCl). Pemalar kekisi dan saiz hablur didapati adalah sensitif kepada perubahan parameter eksperimen. Filem nipis PbS yang diperolehi di bawah syarat-syarat yang optimum

menggunakan plumbum nitrat sebagai sumber ion Pb^{2+}, masa pemendapan 30 min dengan kepekatan molar dalam lingkungan 0.025-0.1 M telah dipilih untuk mengfabrikasikan peranti sel solar PbS/CdS/ITO di bawah keadaan pencahayaan sebanyak 30 mW/cm^2. Peranti sel solar PbS/CdS/ ITO pada kepekatan molar 0.1 M mempunyai kecekapan penukaran tertinggi sebanyak 1.68% berbanding 0.35%, 0.98% dan 1.28%, pada kepekatan molar 0.025, 0.05, dan 0.075 M, masing-masing.

Akhirnya, struktur nano PbS telah disediakan oleh TE dengan menukar suhu pemendapan, jarak antara serbuk dan substrat, dan substrat yang berbeza. Analisis SEM menunjukkan morfologi adalah sangat dipengaruhi oleh parameter di atas. Filem nipis PbS berstruktur nano menghablur dalam struktur jenis garam batuan kubus (NaCl), seperti yang disahkan oleh analisis XRD. Parameter kekisi dan saiz hablur telah didapati sangat sensitif dengan parameter eksperimen. Keputusan menunjukkan bahawa syarat-syarat yang optimum, suhu pertumbuhan 1050°C dan jarak 15 cm dengan substrat yang berbeza membawa kepada penghasilan pelbagai struktur nano. Terumbu karang nano PbS telah digunakan untuk mengfabrikasikan sel solar Schottky PbS/ITO dan memberikan kecekapan sebanyak 0.89%.

FABRICATION OF LEAD SULFIDE (PbS) NANOSTRUCTURES FOR SOLAR CELL APPLICATIONS

ABSTRACT

The main aim of the research work presented in this thesis was to synthesise nanostructured PbS absorber layer for solar cell devices using simple and economical methods: chemical bath deposition (CBD), microwave assisted chemical bath deposition (MACBD) and thermal evaporation (TE). The synthesis of nanostructured PbS layers using CBD was carried out by changing Pb^{2+} ions source, deposition time, and molar concentration. The results showed that the morphology and size-scale of nanostructured PbS features are highly dependent on each parameter. X-ray diffraction analysis (XRD) analysis revealed that all nanostructured PbS thin films exhibit a cubic rock salt (NaCl) type structure. The optimal condition to synthesise nanostructured PbS using CBD was lead nitrate as Pb^{2+} ions source with 0.1M molar concentration. The PbS sample with optimum conditions was selected to be used as an absorber layer on the PbS/CdS/ITO solar cell device.

After that, nanostructured PbS was deposited by MACBD under different conditions: changing Pb^{2+} ion source, varying the deposition time in the range of 30 up to 90 min, and changing the molar concentration. Scanning electron microscopy (SEM) analysis shows that each parameter has effect on morphology changes. Crystal structure analysis by XRD confirms the formation of singularity cubic phase with rock salt (NaCl) type structure. The lattice constants and the crystallite size were observed to be sensitive to the variation of experimental parameters. PbS thin films obtained under optimum conditions using lead nitrate as Pb^{2+} ions source, a deposition time of 30 min with molar concentration in the range of 0.025 - 0.1 M

were selected to fabricate PbS/CdS/ITO solar cell device under the illumination condition of 30 mW/cm^2. PbS/CdS/ITO solar cell device at 0.1 M molar concentration possesses the highest conversion efficiency of 1.68% compared to 0.35%, 0.98%, and 1.28%, at molar concentration of 0.025, 0.05, and 0.075 M , respectively.

Finally, PbS nanostructures were prepared by TE by changing deposition temperature, distance between powder and substrates, and different substrates. SEM analysis shows that the morphology was greatly affected by the above parameters. All nanostructured PbS thin films crystallizes within a cubic rock salt (NaCl) type structure as confirmed by XRD analysis. The lattice parameter and the crystallite size were found to be very sensitive with experimental parameters. The result show that the optimum conditions, a growth temperature of 1050°C and a distance of 15 cm with different substrates led to produce various nanostructures. The obtained nanocoral PbS was used to fabricate PbS/ITO Schottky solar cell and gives an efficiency of 0.89%.

CHAPTER 1: INTRODUCTION

1.1 Overview of nanostructures

In recent years, increased growth has been recorded in the area of research and development of nanostructure science and technology worldwide. Nanostructured materials are classified as those materials with at least one dimension falling within the nanometer scale [1]. Examples are nanoparticles, nano clusters, nano crystals, quantum dots and thin films. Nanostructured materials have gained recognition lately for their unique physical and chemical properties that are broadly different from those of their bulk phases [2, 3].

Nanostructured material are new class of material with greatest potential of improved performance, its properties is outstandingly different from their bulk counterparts and are entirely new class of materials [3, 4]. Their distinctiveness is due partly to the very large percentage of atoms at interfaces and partly to quantum confinement effects. The cooperative interactions produces physical properties recognized as characteristic of bulk materials. The resulting particles always have dimensions in 1nm to 100 nm range. Different sizes mean different band gaps, absorptions and emissions.

The properties of the materials such as electronic, magnetic, optical, and structural can be modified through the adjustment on the sizes of the material. The effect of changes in sizes of nanostructure on its properties has been investigated [5-8]. Quantum confinement is the source of electronic and optical properties of semiconductor nanostructure meaning that the electronic charges are confined to the radius of quantum dots, which is equal to or less than the Bohr exciton radius. Due to this, the valence and conduction band split into discrete levels, and the excitonic

band edge shifted towards higher energies which led to increased molar absorption coefficient with decreased size [9-11]. Modification of the composition, the size, and shape, gives improved properties of nanostructure.

Development of new nanostructured materials have been made possible through the improvements in the colloidal synthesis of inorganic semiconductor nanostructure [12]. This has made possible the use of nanostructured materials in optical switches, solar cells, light emitting devices, photodetectors, and biological labeling.

1.1.1 Quantum size effects

The optical response of a semiconductor wholly depends on its energy band gap (E_g) which controls the threshold energy for an electronic transition from the valence band to the conduction band [13]. In molecular terms, such transition would be equivalent to the lowest energy electronic transition where an electron in the highest occupied molecular orbital is promoted to the lowest unoccupied molecular orbital. The difference in energy between the highest occupied molecular orbit and that of the lowest unoccupied molecular orbit increases as the size of a semiconductor nanocrystal decreases below the critical limit [14]. The properties of the bulk can be expressed in a typical molecular solid as the sum of the individual molecular contributions. The intra-molecular covalent bonding energies are considerably stronger than the intermolecular van der Waals forces. Due to their relatively tiny nature, these intermolecular interactions are prone to slight agitations that rarely extend beyond the nearest neighbor [14, 15].

The size of the crystal will have no effect on the electronic properties of the crystal under such condition. Inorganic semiconductors have no discrete molecular

unit; they are made up of network with well-arranged atoms that interact throughout the entire lattice through strong chemical bonds. The absorption of an optical photon leads to the production of a Mott-Wannier exciton in a bulk semiconductor crystal [16]. This electronic excitation consists of a loosely bound electron-hole pair which is delocalized over a certain length, typically larger than the lattice constant, known as the Bohr radius [17-19]. Quantitatively, the Bohr radius a_B, can be expressed as:

$$a_B = \frac{\hbar^2 \varepsilon}{e^2}\left(\frac{1}{m_e^*} + \frac{1}{m_h^*}\right) \tag{1.1}$$

where $\hbar = \frac{h}{2\pi}$, h is Planck's constant, e is the fundamental electronic charge, ε is the bulk dielectric constant, and m_e^* and m_h^* are the effective masses of the electron and hole, respectively. In materials of higher dielectric constant, Coulomb attraction between the electron and hole is more effectively suppressed and delocalization is enhanced [20].

The two basic factors that distinguish the behavior of nanocrystal from the corresponding macro crystalline materials depend on the size of individual nanocrystal. There is a high dispersity (large surface/volume ratio) associated with the particles, while the physical and chemical properties of the semiconductor are sensitive to the surface structure. Secondly, the actual size of the particle plays a significant role in determining the electronic and physical properties of the material. Reduction in size of the semiconductor crystal leads to the determination of Bohr radius, quantum confinement and the optoelectronic properties get modified [17, 18]. The electron and hole show more compaction in nanometer sized particles than in the macro crystalline material, and as a result there is a strong Coulomb interaction

between electron and hole; they have higher kinetic energy than in the macro crystalline material.

The effect of three-dimensional confinement is that it collapses the continuous density of states of the bulk solid into the discrete electronic states of the nanocrystal [13]. The finite size of the nanocrystal quantizes the allowed k values. Decreasing nanocrystal diameter shifts the first state to larger k values and increases the separation between states. Several models have been proposed to explain the dependence of exciton energy on cluster size [21-24]. Brus showed that for strongly confined systems, the size dependence on the energy of the first electronic transition of the exciton can be approximately calculated using

$$\Delta E \cong \frac{h^2\pi^2}{2R^2}\left(\frac{1}{m_e^*}+\frac{1}{m_h^*}\right)-\frac{1.786e^2}{\varepsilon R} \qquad (1.2)$$

where R is the radius of the particle [22]. The first term in Equation 1.2 contains the familiar $\frac{1}{R^2}$ dependence associated with the particle in a box treatment and shows the energy shift due to quantum localization. The second term depicted in Equation 1.2 shows $\frac{1}{R}$ dependence and is representative of the Coulomb interaction energy. The predicted behavior of Equation 1.2 has been confirmed experimentally for a wide range of semiconductor nanocrystallites, with a blue shift in the onset of absorption of incident light being observed with decreasing particle diameter. Equations 1.1 and 1.2 are widely used and are believed to contain the fundamental physics involved in the quantum confinement effect.

The charge carriers' confinement in nanostructures reduces their degree of freedom. Carrier confinement and reduced dimensionality are described by the energy dependence of the density-of-states (DOS), or the number of states per unit energy. There is a large variation in the energy required in adding or in removing charges from a nanocrystal because of their optical and electrical properties, which are size dependent [25]. The spectrum of single-particle states is a set of sub-bands having one or two-dimensional states in the quantum well (confinement is taken along the z-directions) and in the quantum wire (confinement is taken along the yand z-directions). The separation between sub-bands, which is a continuum of states, is determined by the splitting between the levels for the confined motion. When splitting increases with an increase in confinement, well size decreases and barrier height increases. The electron-hole pair becomes frozen in the lowest-energy singleparticle states when confinement is increased in a quasi-zero dimensional structure quantum dot (DOS) (confinement is taken along the x, y, and z-directions). DOS is a set of discrete states [68]. The level splitting scales is described as 1/L2, where L is the size of the quantum dot. The Coulomb energy scale is 1/L, as shown in Figure 2.1.

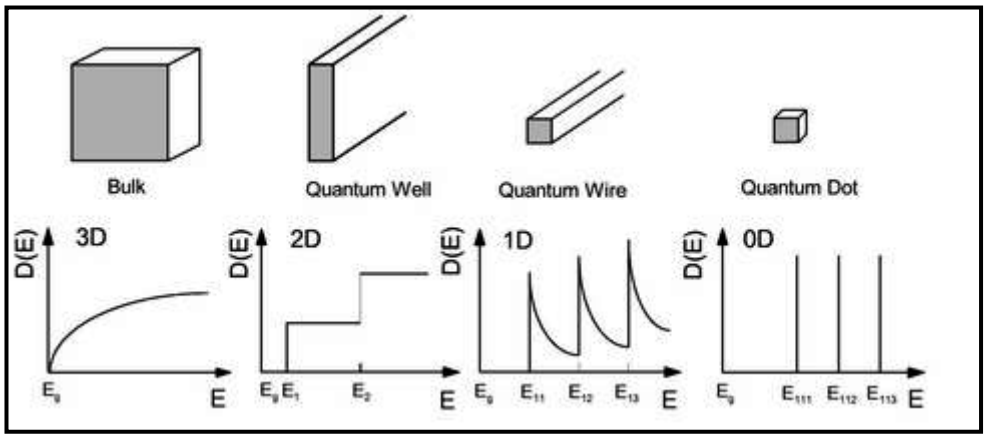

Figure 1.1: Density-of-states for different low-dimensional structures. Adopted from [25].

However, they lack in two important aspects. First, the energy bands can significantly deviate from the assumed parabolic character, and typically more so as the size of the particle is reduced. This deviation from parabolic behavior can also be especially evident in materials possessing a relatively small band-gap. This implies that the effective mass approximation is no longer valid except in the region where k = 0. Secondly, while the structures found in nanocrystals are often quite similar to those observed in the corresponding bulk materials, the differences could significantly change the effective masses of the electrons and holes.

1.2 Overview and background of PbS

Lead sulfide (PbS) comprise narrow band gap semiconductors. Their crystal structure is face centered cubic with a coordination number of six. The bond between Pb and S is generally considered to be ionic [25] as shown in Figure 1.1. The minimum energy gap, (E_g) , between the conduction band and the valence band is a direct narrow optical energy gap (0.41 eV at 300K) with relatively large excitation Bohr radius of 18 nm. These properties account for the strong quantum confinement of both electrons and holes in nanosize structure [26]. Therefore, the value of the band gap can be adjusted through the modification of the particle size and shape, according to the effective mass model [27-29]. Lead sulfide has many distinct features compared to other semiconductors [25]. Their band gaps are smaller at room temperatures, implying that the temperature coefficients of (E_g) are positive and negative for all other compound semiconductors such as Si.

Their lattice structure may be very unstoichiometric. The vacancies and interstitials control the conductivity type. For example, an excess of Pb and chalcogenide causes n-type conductivity and p-type conductivity respectively.

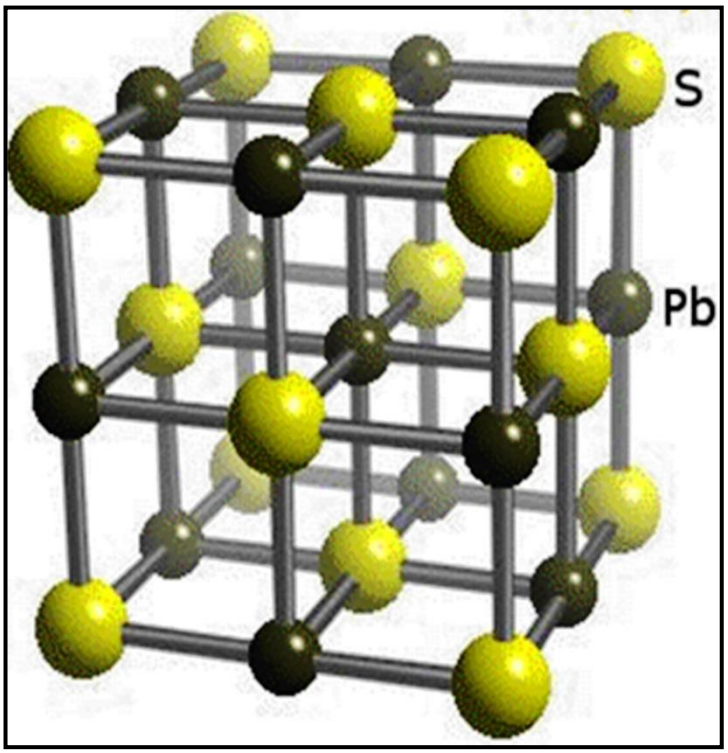

Figure 1.2: Cubic crystal structure of PbS. Adopted from Ref [30].

This property of PbS allows for its use in infrared (IR) detectors, electroluminescent devices, solar cells, and other optoelectronic devices [30]. Hence, there has been rising interest in developing novel processing routes for the preparation of PbS at the nanoscale especially as thin films.

Over the years, lead sulfide thin films have been prepared using several gas phase methods, and they include: molecular beam epitaxy (MBE) [31-33], hot wall epitaxy (HWE) [34-36], sputtering [37, 38], chemical vapour deposition (CVD) [39-45], and atomic layer epitaxy (ALE) [46, 47]. Liquid phase techniques include

electrodeposition [48-51] and successive ionic layer adsorption and reaction (SILAR) [52-55].

Chemical bath deposition (CBD) is the oldest and the most researched PbS thin film deposition method. It was used to deposit PbS as far back as 1910 [56]. CBD is used to make the PbS films in commercial IR detectors. CBD method has become an important method for the preparation of thin films because of several inherent benefits which include; industrial-scaled manufacturing, low cost, appropriateness for large scale deposition areas, ability to deposit thin films on different substrates, and flexibility of tuning thin film properties simply by controlling and adjusting the deposition experimental parameters [57].

Several efforts have been made in the recent times to grow PbS thin films using CBD technique. Pentia et al., synthesized nanocrystalline PbS using CBD to study the electrical and photoelectrical properties and the difference between "standard" and "nanocrystalline" film [58]. They concluded that the shift of the maximum of photosensitivity to shorter wavelengths and the larger value of Eg depend on the nanoparticles size effect. Larramendi et al., studied the effect of adding KBr to the deposited solution [59]. Their study confirmed that surface morphology can be altered with resulting changes in optoelectric features of the film, though depending on its concentration in the solution. Salim et al., also deposited PbS thin films by chemical deposition on a glass substrate to study the morphology, optical, and electrical properties of the as-deposited and heat-treated films [60].

Lopez et al., used impedance spectroscopy to acquire electrical and structural information of chemically deposited CdS and PbS polycrystalline thin films [61]. Pentia et al., showed that the IR photoconductive properties of PbS films could be controlled using chemical and physical methods [62]. Joshi et al., used chemical bath

deposition method to fabricate the PbS nanoparticle on glass, quartz and silicon substrates [63]. They discovered that decreased grain size will increase the optical band gap. Zhang et al., prepared PbS nanocubes and PbS dendrites crystal using a complex solvothermal synthetic method [64].

Popa et al., prepared nanocrystalline PbS thin films on glass substrates using CBD method, and measured the crystal size by optical absorption and photocurrent measurements [65]. Zhao et al., prepared dentritic-like PbS nanostructures using lead acetate trihydrate, thioacetamide (TAA), and nitrilotriacetic acid as precursors without any surfactants by ultrasonic method [66]. Jana et al., grew nanoparticles of PbS within the pores of polyvinyl alcohol (PVA) matrix on glass substrates using the CBD technique at a temperature below room temperature (30 °C) [67]. Popescu et al., analysed a number of electrical and photoelectrical properties of PbS obtained by sonochemical static or ultrasonic (US) baths as a function of the deposition condition [68]. The study discovered that increasing the reaction rate with ultrasound leads to thicker films with smaller electrical resistance. Barote et al., utilized CBD to prepare N-type PbS by mixing with polymer, to study photoelectrochemical properties [69]. Preetha et al., studied the effect of pH on optical and transport properties of SILAR deposited nanocrystalline PbS thin films [55].

Previous studies worked on the effect of time deposition on the synthesis of PbS thin films [70-73]. The studies showed that the morphology, structural, and optical properties were very sensitive to the change of deposition time. Seghair et al., [74], Choudhury et al., [75], and Choudhury et al., [76] studied the effect of using different ion sources and different molar concentrations, where they found that lead acetate showed more potential than lead nitrate. Ramírez et al., [77], Qadri et al., [78], Abdel Rarea et al., [79], and Abbas et al., [80] worked on effect of synthesizing

PbS thin films using CBD at different temperatures. These studies were conducted using different laboratory tools of measurement.

Generally, the preparation of PbS films using CBD method require low temperature and a lengthy processing duration [27, 58]. In addition, microwave irradiation is usually used to prepare organic and inorganic materials. When a material is exposed to electromagnetic wave, it will absorb the electromagnetic energy and transform it into thermal energy [81, 82]. In this case, heat is generated from inside the material through the microwave irradiation, whereas in other methods, heat is usually transmitted from the outside of the material to the inside. Hence, the production of internal heat reduces the reaction time and energy cost, as well as allow as the synthesis of new material [83, 84].

Therefore, the integration of microwave irradiation and chemical bath deposition is referred to as microwave assisted chemical bath deposition (MACBD). It is generally rapid, uncomplicated and energy-efficient. MACBD synthesis method has been extensively used in the synthesis of PbS nanocrystals by different studies [85-88]. Attention has been focused on depositing PbS using microwave assisted chemical bath deposition because of its ability in producing good crystalline guality of nanostructured PbS thin films with improved optical properties [89]. Coa et al., used microwave-assistant heating method to synthesize hierarchical architectures of PbS with ethylene glycol (EG) as solution, and obtained different morphologies, e.g., cubic particles, six arms, and bugle-like dendrites [90].

Phuruangrat et al., reported a study on the synthesis of PbS from different Pb^{2+} and S^{2-} ions sources in propylene glycol using a cyclic microwave radiation at different powers and prolonged times [91,92]. Sun et al., prepared PbS crystals with flower-like morphology in ethylenediamine by microwave thermolysis of a single-

source molecular precursor of lead diethyldithiocarbamate [93]. Jayesh et al., carried out a study on controlled morphology and size of PbS by capping PbS nanoparticles with PVA using microwave assisted chemical bath deposition [94].

PbS can be prepared as different nanostructures using thermal evaporation (physical vapor deposition technique), via the solid-vapor deposition (VS) mechanism. One of the key benefits of this method is that the operating parameters can be chosen from a broad range, resulting in a great variety of film structures [95].

For example, lead chalcogenide nanostructure has been synthesized using the thermal evaporation process. Kumar et al., synthesized PbS thin films on ultra-clean glass substrates by vacuum evaporation technique, and fabricates Schottky junction of PbS semiconductor with indium metal [96]. The same group also synthesized polycrystalline thin films of $PbS_{1-x}Se_x$ with variable composition $(0 \leq x \leq 1)$ and deposited the films on ultra clean glass substrates by vacuum evaporation technique [97]. In addition, Kumar et al., synthesized polycrystalline lead chalcogenides thin films on optically plane and chemically clean glass substrates using the vacuum evaporation technique [98]. Salim et al., studied the structure and optical properties of bismuth sulfide-lead sulfide $[(Bi_2 S_3)_{1-x} (PbS)_x]$ [99]. The thin films were prepared by thermal evaporation on glass substrate from powder $(Bi_2 S_3)_{1-x} (PbS)_x$, at different ratios of x $[0.1 \leq x \geq 0.85]$. Kumar et al., investigated the properties of solid solutions of pseudo-binary lead chalcogenides when deposited onto ultra clean glass substrates by vacuum evaporation technique [100].

However, these studies were conducted with different parameters under varying conditions. More so, the processes in all the studies used high-purity commercial powder, different diffusion temperature, and diverse tools of

measurement. As a result, solid-vapor synthesis of nanostructures metal sulfides without the aid of templates and catalysts have not been studied comprehensively.

1.3 Overview and background of CdS

Cadmium sulfide (CdS) is one of the most essential II–VI semiconductors, with direct band gaps of 2.42 eV and 2.57 eV in cubic phase and hexagonal phase respectively [101], although the exciton Bohr radius of CdS is only 2.8 nm [102]. CdS is an important wide band gap semiconductor due to its wide range of applications, particularly in the formation of optoelectronic devices such as tunable light emitting diodes and in the manufacture of highly efficient solar cells, usually by coupling with other materials [103,104].

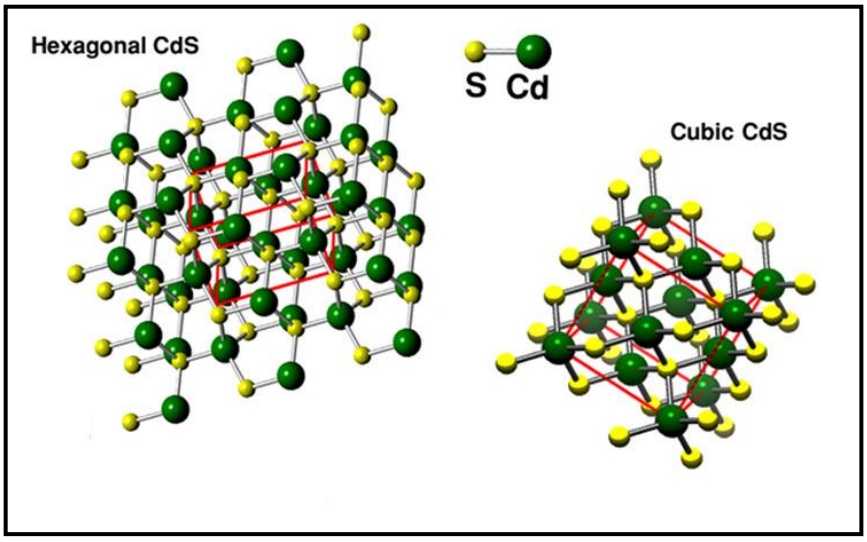

Figure 1.3: Crystal structure of CdS. Adopted from [105].

Various methods have been used basically to synthesize CdS thin films, such as chemical vapor deposition (CVD)[106], molecular beam epitaxy MBE [107],thermal evaporation (TE) [108], pulsed laser deposition [109], spray pyrolysis deposition (SPD) [110-112], electrodeposition (ED) [113,114], sol-gel [105], and chemical bath deposition (CBD) [115-119]. CBD is typified by simple formulation

system, low temperature requirement and simple control of the thin film properties under different deposition conditions.

Therefore, CBD is preferred as an attractive method because of its large scale deposition, and capability to deposit on different substrates [120]. The complex composition of thin films prepared using the CBD method causes low crystallinity, which limits their use in certain applications. Hence, microwave irradiation was utilized as the heat source during CBD to synthesize high-quality CdS nanocrystalline thin films with enhanced optical properties. The application of microwave irradiation in the preparation of nanosized CdS have been reported in contemporary studies.

Zhu et al., prepared nanoparticles of CdS, ZnS using the reaction between $CdCl_2$ or $Zn(Ac)_2$ and thioacetamide in aqueous solution with microwave irradiation as the heat source [121]. Zhu et al., reported the preparation of CdS nanoribbons by the microwave irradiation of an ethylene diamine solution of 1-pyrrlidine dithio carboxylic acid ammonium salt (APDTC) and cadmium chloride under ambient air [122]. Chen et al., studied the preparation of nanocrystalline metal sulfides by a rapid reaction between metal salts and thiourea in ethylene glycol (EG) under microwave irradiation [83]. Singh et al., synthesized CdS for solar cell applications using sonochemical and microwave-assisted hydrothermal method [123]. Zhang and Gao reported the synthesis of CdS nanorods using hydrothermal microemulsions, and they observed that altering some factors in the synthesis path such as temperature and surfactant type provided a means to direct the shape and size of the particles [124]. Zhai et al., used MACBD method that had been developed for the fabrication of CdS and ZnS thin films [125]. Liu et al., used MACBD to fabricate micro/nano-binary

structures of CdS thin films [126]. The study suggested the ion-by-ion mechanism to form a layer of nanocrystalline film on the substrate surface while layers of CdS aggregations were formed in the solution based on the cluster-by-cluster mechanism. Furthermore, Oliveira et al., synthesized nanocrystalline CdS with different morphologies (flowerlike nanostructures, and nanoplates) using a microwave-assisted solvothermal method [127].

Among the several n-type semiconductor materials, it has been noted that nanocrystalline CdS is the most potential heterojunction partner for the polycrystalline photovoltaic material as a window layer material for n-CdS/p-type solar cell materials. Light can penetrate through the n-type CdS layer and be absorbed in the p-type layer. The induced electron–hole pairs are then divided in the depletion region of the n-CdS/p-type materials heterojunction. Thus, it is evident that the CdS layer is a crucial factor in the improvement of photovoltaic performance [128]. This implies that the electrical, optical and structural properties of the CdS layer can affect the performance of the whole cell considerably. To prevent the short circuit effects, the CdS layer should be thin, uniform and conductive to permit high transmission.

Several studies have explored other fabrication techniques for attaching CdS window layer. Petillon et al., examined the growth of CdS/ZnSe type II quantum-well structures, produced by MBE on GaAs (001) substrates [129]. Boieriu et al., prepared epitaxial layers of wurtzite CdS on CdTe $(\bar{1}\bar{1}\bar{1})$ /Si substrates using molecular beam epitaxy, while indium was used to acquire n-type doping of CdS [130]. Rusu et al., studied the optimization of the CdS chemical bath deposition process to be applied to solar cells based on polycrystalline CuGaSe2 (CGSe) absorber layers prepared in two stages by physical vapour deposition [131]. Romeo

et al., used sputtering to prepare CdS window layer for CdTe/CdS solar cell [132]. Li et al., showed the dependence of absorption wavelength on the well width in (CdS/ZnSe) / BeTe super lattices (SL) formed on GaAs substrate by MBE [133].

Zhu et al., investigated the efficient inverted polymer solar cell (PSC) by utilizing an atomic layer deposited (ALD) CdS film between the indium tin oxide (ITO) cathode and the photoactive electron collection layer (ECL) [134]. Perrenoud et al., fabricated CdTe/CdS and CdTe/ZnO thin film solar cells using a high vacuum evaporation based low temperature process (≤ 420 °C) [135]. Zhang et al., synthesized CdS window layer grown by SILAR processes for CdS/CdSe co-sensitized TiO_2 solar cells [136]. Zhang et al., fabricated Bi_2Se_3 and CdS co-sensitized TiO_2 nanorod (NR) arrays photoelectrode using the CVD method [137].

Abou-Ras et al., examined the structural and chemical properties of CBD- and PVD-CdS buffer layers and interfaces in $Cu(In,Ga)Se_2$ based thin film solar cells [138]. Vigil-Galán et al., conducted a study to enhance the efficiency of CdS/CdTe solar cells by changing the thiourea/$CdCl_2$ ratio in the chemical bath solution employed for the deposition of the CdS layers. They found that the optimum ratio for the deposition of CdS films is (5), because the films obtained demonstrate better optical and structural characteristics [139]. Estela Calixto et al., carried out a study on chemical bath deposited CdS bi-layers. The process involves the deposition of a CdS layer at 75 °C for 10 min accompanied by a second CdS film at 40 °C for 45 min to form the bi-layer [140]. Nair et al., suggested CdS thin films as a window layer in solar cell structures (CdS/Sb_2S_3/PbSe) [141]. The cells are prepared by the sequential chemical deposition of the films on a commercial SnO_2: Float coated sheet glass. Han et al., prepared CdS layers grown by ‘dry’ (close space sublimation) and

'wet' (chemical bath deposition) methods for CdTe solar cell. CdS prepared with close space sublimation (CSS) show enhanced crystalline, electrical and optical properties than that prepared using CBD methods [142]. The performance of CdTe solar cell based on the CdS layer has a higher efficiency compared to that based on CBD CdS layer. Joshi et al., prepared CdS thin films by CBD method on conducting ITO coated glass substrates for heterojunction solar cell of CdS/$CuInS_XSe_{2-X}$ [143]. Hernandez et al., reported on study of nanostructured solar cell with glass/ITO/CdS/PbS/conductive graphite structure [144]. Both window (CdS) and absorption (PbS) layers were deposited by means of the CBD technique. Harumi et al., reported on solar cells with a cross-sectional layout: transparent conducting oxide (TCO)/window/Bi_2S_3/PbS, where a commercial SnO_2 was used as transparent conductive oxide (TCO), while CdS, and ZnS were used as window layers [145].

However, increased efficiency should be attained by employing nanocrystalline CdS as a window layer for solar cell applications. The general decrease in optical absorption due to the blue shift can result in higher performance, particularly in short-circuit currents in solar cells. This provides a better window material than bulk CdS, therefore many studies have created a microwave-hydrothermal method to fabricate CdS window layer. Singh et al., prepared CdS films on indium tin oxide (ITO)/glass using sonochemical and microwave methods, made with solution grown CdS films on ITO/glass [123]. Zhu et al., utilized an uncomplicated, fast and effective method of MACBD methods to synthesise CdS quantum dots on the surface of TiO_2 film resulting in a photo anode of quantum dot-sensitized solar cells [146]. Zhu et al., reported on CdS/CdSe quantum-dot (QD) co-sensitized TiO_2 film which has been fabricated using MACBD methods and used as a photoanode for QD-sensitized solar cells [147]. Same group also studied sensitized-

type solar cells based on TiO_2 photoanodes and CdS quantum dots (QDs) as sensitizers using MACBD methods [148]. Yang et al., synthesized CdS sensitized TiO_2 electrodes using MACBD methods [149]. After an extensive literature review, it can be concluded that no study has been reported for fabrication of CdS/PbS solar cell by employing microwave-irradiation technique. This is the main motivation behind the current studies investigating the effects of MACBD method on the fabrication and characterization of CdS/PbS heterojunction solar cells.

1.4 Motivation for this research

Presently, the world's energy needs are rising gradually. However, the conventional sources of energy are limited. Solar energy such as photovoltaic energy (PV) is the most accessible energy source capable of meeting this world's energy requirements. The conversion of sunlight into electricity using solar cells system is a valuable way of producing this alternative energy. The search for renewable energies has been a passion for researchers all over the world. The use of nanostructured materials has offered significantly enhanced features lacking in other materials, such as light absorption and charge separation, which are the two crucial aspects of solar-to-electric energy conversion. In thin film technologies, there exists a general difficulty with conversion efficiency due to poor material quality; thus the photo-generated electrons and holes are unable to travel long distances before recombination (short free-carrier diffusion lengths) and are hence lost to power conversion. Such problem could be resolved by fabrication of solar cell on nanostructured material. This property will reduce the distance required for photo-generated carrier, as well as the reduction of unwanted recombination. The main reason for nanostructuring is to develop a device that is optically thick to efficiently

absorb the incident sunlight, and at the same time have every photogenerated electron-hole pair be very close to the p/n junction with respect to the minority carrier diffusion length, in order to reduce recombination losses.

It is vital to know that over the years, highly efficient and cheap fabrication of solar cells pose a challenge to scientific research due to the material production and fabrication process. These include increasing efficiency in order to reduce the amount of solar cells needed, and developing technologies with lower operational and material costs. The most apparent approach to reduce the amount of materials consumed, and the cost of the fabrication process are solutions being developed in this research. In this study, inorganic nanostructures (NCs) were used in order to decrease the amount of manufacturing material used. NCs are potential materials to fulfill these requirements since their band gap is widely tunable to a preferred wavelength by basically controlling the NCs` size during the process of synthesis. The thin CdS (300nm) layer was used as the window layer. For the active layer (0.985– 1.4 μm), PbS can be deposited using different methods; CBD and MACBD which are cheap and economical methods, were used to deposit the layers. The second option seeks to cut down the cost of the fabrication process. Low cost and simple thermal evaporation technique was used to deposit PbS layer for Shottky solar cell. Several studies have improved the technology through different phases by increasing the efficiency of the devices and reducing fabrication costs. Further work will emphasize on both efficiency and increased film-deposition rates to produce economical modules.

1.5 Research objectives

The principal objectives of this project are summarized in the following points:

1. To study PbS nanostructures synthesised using chemical bath deposition (CBD) under different conditions

2. To investigate PbS nanostructures synthesised using simple, low cost, and clean microwave assisted chemical bath deposition techniques under different conditions

3. To analyse PbS nanostructures prepared under different conditions using thermal evaporation

4. To investigate the properties of PbS/CdS solar cell fabricated using low cost CBD and MACBD techniques, and PbS Schottky solar cell fabricated using thermal evaporation technique.

1.6 Thesis organization

The thesis is organized into seven chapters. Chapter 1 consists of an overview of literatures on the properties and deposition of PbS and CdS. Chapter 2 presents the general principles and theories of the chemical bath deposition (CBD), microwave assisted chemical bath deposition (MACBD), thermal evaporation (TE), principles and mechanism of PbS and CdS preparations, and the basic principles of some devices which were fabricated for this thesis. Chapter 3 entails the methodology and instrumentation of experiments conducted in the research. The results obtained from the research are analyzed and discussed in the next three chapters. Chapter 4 focuses on the properties and preparation of nanostructured PbS using CBD under different conditions, and its applications to the CdS /PbS solar cell structure. Chapters 5

elucidates on the synthesis of the PbS nanostructures and discusses the fabrication of the CdS/PbS solar cell using MACBD. Chapter 6 present the synthesis of PbS nanostructures using thermal evaporation (TE) under different conditions, and Chapter 7 presents a brief discussion of the findings of this work and future opportunities.

CHAPTER 2: THEORY

2.1 Introduction

The general principles and theories involved in this study are presented in this chapter. The chapter begins with a brief explanation of the principles of CBD and the mechanism of lead sulfide (PbS) formation. The fundamentals of MACBD, the mechanism of PbS and cadmium sulfide (CdS) formation, and the fundamental theories of thermal evaporation (TE) are addressed. The basic principles of solar cells, which were fabricated in this study, are also briefly described in this chapter.

2.2 Principle of CBD

The synthesis of nanostructured materials is the key to their practical application, which has attracted much attention in the last decade. Many techniques have been developed to synthesize nanostructured materials, such as CBD. The CBD technique is utilized extensively for the deposition of nanostructured thin chalcogenide films. CBD, unlike other methods, does not require progressive and expensive instruments and equipment; the required chemicals are readily available and cheap.

CBD is a low-temperature deposition method that prevents oxidation; various substrates, including insulators, semiconductors, and metals, can be utilized [150]. This technique has been employed to prepare PbS thin films since the 1910s [8]. The basic principle involved in the synthesis of thin films through the CBD technique is the controlled precipitation of the desired compound from a solution of its constituents. A complexing agent as a component of the bath eliminates spontaneous precipitation by slowing down the release of dissociated metallic ions, thereby

resulting in the slow precipitation of the compound [150]. CBD has become a popular method for many reasons, such as easy operation and low cost, suitability for large-scale deposition areas, ability to deposit thin films on different substrates, and ease in controlling thin film properties by controlling the deposition parameters. The two mechanisms in CBD are ion-by-ion and hydroxide (cluster) mechanisms [151]:

2.2.1 Ion-by-Ion mechanism

The simplest conceptual mechanism often assumed to be the operative mechanism is ion-by-ion mechanism because it occurs by sequential ionic reactions [151]. The basic principle of this mechanism, as illustrated for PbS, is given by

$$Pb^{2+} + S^{2-} \rightarrow PbS \qquad (2.1)$$

The solubility product, K_{sp}, is defined as the solubility product constant. The K_{sp} value will be utilized to describe the saturated solutions of ionic compounds with relatively low solubility [95].

A saturated solution is in a state of dynamic equilibrium between the dissolved, dissociated ionic compound and the undissolved solid [152]. The K_{sp} value for PbS is 4×10^{-28}. PbS can form as a solid phase, although a large ionic product may be required if supersaturation occurs when the ion product, $[Pb^{2+}]\,[S^{2-}]$, exceeds the solubility product, K_{sp}, [150]. If the ion product does not exceed K_{sp}, no solid phase will form except for possible transient local fluctuations in the solution. Small solid nuclei will redissolve before growing into a stable size [151]. Thus, the precipitation process is presented as an equilibrium reaction rather than a one-way reaction. The reasoning that no solid phase will form if the ion product does not exceed K_{sp} may not be true under certain circumstances.

PbS formation could occur on the substrate surface in the condition that none can be formed homogeneously. Equation (2.1) provides the overall reaction for the formation of PbS. However, the process is complicated and comprises a number of reactions and equilibria. The mechanism involves the formation of S^{2-} ions and control of Pb^{2+} concentration. The S^{2-} can be formed from the decomposition of thiourea by aqueous alkaline solution [124].

$$(NH_2)_2CS + 2OH^- \rightarrow S^{2-} + CN_2H_2 + 2H_2O \quad (2.2)$$

The deposition rate can be easily controlled by controlling the rate of reaction (2.2) provided that S^{2-} concentration is as low as desired. (e.g., utilizing low temperatures and/or relatively low pH). The deposition rate can be easily controlled even at relatively high free Pb^{2+} concentrations. An alkaline pH is required to decompose thiourea to sulfide; thus, a complexing agent is needed to maintain Pb^{2+} in the solution and block lead hydroxide [$Pb(OH)_2$] from precipitating [150-153]. The ion-by-ion mechanism is shown in Appendix A. The reaction is completed after some time as indicated by the chocolate color of the solution, which means that the synthesis of PbS is completed by nucleation and growth processes (step C).

2.2.2 Hydroxide (Cluster) mechanism

$Pb(OH)_2$ precipitation should be prevented as mentioned in Section 2.2.1. Precipitation can be prevented by calculating the concentration of required ammonia. In reality, CBD is often performed when metal hydroxide (or hydrated oxide) is formed [152-155]. This condition implies that a precipitate (e.g., $Pb(OH)_2$) is formed at the beginning of the deposition. Otherwise, $Pb(OH)_2$ is formed as a colloid rather

than a precipitate or as an adsorbed species on the substrate and not in the bulk of the solution because $Pb(OH)_2$ is colorless and colloids do not usually scatter light (otherwise, it is a suspension). The PbS is then formed by reaction of S^{2-} ion with the Pb(OH)2 :

$$Pb^{2+} + 2OH^{-} \rightarrow Pb(OH)_2 \quad (2.3)$$

Followed by

$$Pb(OH)_2 + S^{2-} \rightarrow PbS + 2OH^{-} \quad (2.4)$$

The main component of Eq. (2.4) is the much lower Ksp value for PbS (10^{-28}) than that for $Pb(OH)_2$ (10^{-15} to 10^{-20}), which reflects the presence of high negative free energy in the formation of PbS [120]. This condition indicates that sulfide can readily substitute for hydroxide in the case of Pb. The amount of sulfide required to convert $Pb(OH)_2$ into PbS can be calculated from the ratio of the two solubility products.:

$$\frac{K_{sp}\ (PbS)}{K_{sp}\ (Pb(OH)_2)} = \frac{[Pb^{2+}][S^{2-}]}{[Pb^{2+}][OH^{-}]_2} \quad (2.5)$$

The value of $[S^{2-}]$ is 5×10^{-21}M at a pH of 11 ($[OH^-]$ 10^{-3} M at room temperature) [154]. Thus, a very low concentration of S^{2-} is required to convert $Pb(OH)_2$ into PbS. Considering that most of the sulfide species are in HS rather than S, the $[S^2]$:[HS] ratio is 10^{-7} and the required HS concentration is 10^{-14} M at pH 11. The HS concentration is still a very low concentration [152]. The OH concentration is about an order of a magnitude higher at high temperatures because of the strong temperature dependence of the ionic product of water. The required S^{2-} concentration